Annals of Botany **123**: 1205–1218, 2019
doi: 10.1093/aob/mcz027, available online at www.academic.oup.com/aob

ANNALS OF BOTANY
Founded 1887

Mimicking pollen and spore walls: self-assembly in action

Nina I. Gabarayeva*, Valentina V. Grigorjeva and Alexey L. Shavarda

Komarov Botanical Institute, Popov St. 2, 197376, St Petersburg, Russia
**For correspondence. E-mail 1906ng@mail.ru*

Received: 5 October 2018 Returned for revision: 23 January 2019 Editorial decision: 11 February 2019 Accepted: 14 February 2019

• **Background and Aims** Decades of research have attempted to elucidate the underlying developmental mechanisms that give rise to the enormous diversity of pollen and spore exines. The organization of the exine starts with the establishment of an elaborate glycocalyx within which the subsequent accumulation of sporopollenin occurs. Ontogenetic studies using transmission electron microscopy of over 30 species from many different groups have shown that the sequence of structures observed during development of the exine corresponds to the sequence of self-assembling micellar mesophases (including liquid crystals) observed at increasing concentrations of surfactants. This suggested that self-assembly plays an important part in exine pattern determination. Some patterns resembling separate layers of spore and pollen grain walls have been obtained experimentally, *in vitro*, by self-assembly. However, to firmly establish this idea, columellate and granulate exines, the most widespread forms, needed to be simulated experimentally.
• **Methods** We used our original method, preparing mixtures of substances analogous to those known to occur in the periplasmic space of developing microspores, then leaving the mixtures undisturbed for specific periods of time to allow the process of self-assembly to occur. We developed our method further by using new substances analogous to those present in the periplasmic space and performing the experiments in a thin layer, more closely resembling the dimensions of the periplasmic space.
• **Key Results** The artificial microstructures obtained from our *in vitro* self-assembly experiments closely resembled the main types of exines, including tectate–columellate, granulate, alveolate and structureless, and permitted comparison with both developing and mature microspore walls. Compared with the previous attempts, we managed to simulate columellate and granulate exines, including lamellate endexine.
• **Conclusions** Our results show that simple physico-chemical interactions are able to generate patterns resembling those found in exines, supporting the idea that exine development in nature involves an interplay between the genome and self-assembly.

Key words: Modelling of pollen and spore walls, mechanisms of development, micelles, self-assembly.

INTRODUCTION

The idea of the universal importance of self-assembly for pattern formation in nature is an old one (Thompson, 1917) and has been elaborated on by many authors (e.g. Ingber, 1993; Kauffman, 1993; Kurakin, 2005; Benítez, 2013). As Mandelbrot (1982, p. 162) put it, 'Characteristics preordained by geometry need not burden the genetic code'. Contemporary studies (Lintilhac, 2014) confirm that biophysically integrated controlling processes provide an independent, non-genetic context for understanding plant morphogenesis, and that physical forces play a prominent role in development.

Wodehouse (1935) was the first to apply Thompson's (1917) ideas on pattern determination to pollen morphological diversity. The more facts that accumulate, the more it appears that self-assembly processes cooperate with and modify the regular work of the genome (Heslop-Harrison, 1972; Gerasimova-Navashina, 1973; Sheldon and Dickinson, 1983; Dickinson and Sheldon, 1986; Gabarayeva, 1990, 1993; van Uffelen, 1991; Hemsley *et al.*, 1992; Collinson *et al.*, 1993; see also the review of Blackmore *et al.*, 2007). Despite many genes playing a role in exine establishment (e.g. Ariizumi and Toriyama, 2011; Dobritsa *et al.*, 2011; Quilichini *et al.*, 2015), the reiteration of exine patterns (e.g. reticulate, columellate, white-lined lamellae) suggests that these patterns are based on some non-biological principles of space-filling operations (Scott, 1994). Our studies of sporoderm ontogeny in more than 30 species from a wide variety of taxa (Gabarayeva, 1991, 2014; Gabarayeva *et al.*, 2009, 2010*a*, *b*, 2011*a*, *b*, 2013, 2016, 2017, 2018*a*, *b*; Gabarayeva and Grigorjeva, 2010, 2011, 2012, 2014; Grigorjeva and Gabarayeva, 2015) have revealed recurrent sets of structures, observed during the course of exine development, with species-specific final exine patterns revealing themselves at the middle free microspore stages. This fact could not be ignored, and our early supposition was that the glycocalyx (*syn.* primexine matrix) is a colloid, and that self-assembly is important in exine development (Gabarayeva, 1990, 1993). Concurrently, the iridescent crystalline structure of *Selaginella galeottii* and *Erlansonisporites* sp. megaspore walls put Hemsley and his group onto the same idea (Hemsley *et al.*, 1992, 1994), defining it more precisely as micellar self-assembly (Collinson *et al.*, 1993). Indeed, if the glycocalyx consists of surface-active substances, the sequence of self-assembling structures would be predicted to appear in the periplasmic space. The established facts are that glycoproteins and lipopolysaccharides (most

of which are surface-active) are initially dispersed in hydrophilic liquid within the narrow periplasmic space (Rowley, 1971, 1975; Pettitt and Jermy, 1974; Rowley and Dahl, 1977; Pettitt, 1979). Later in the tetrad stage, other surface-active substances, such as sporopollenin lipoid precursors and monomers – fatty acids, aromatic units, especially *p*-coumaric acid (Gubatz *et al.*, 1986; Wehling *et al.*, 1989; Gubatz and Wiermann, 1992; Wilmesmeier and Wiermann, 1997; Niester-Nyveld *et al.*, 1997; Grienenberger *et al.*, 2010; Legrand, 2010; Wang *et al.*, 2013; Quilichini *et al.*, 2015) and aliphatic units (de Leeuw *et al.*, 2006) – are added to the periplasmic space. A recent, long-anticipated paper on the chemical composition of sporopollenin and its precursors and monomers has greatly enriched our knowledge on the topic (Li *et al.*, 2019) and confirmed many of the earlier findings of Wiermann and others, especially concerning such monomeric building blocks as fatty acid derivatives and phenolics (*p*-coumaric acid monomers). Being colloid systems of surface-active substances, developing exines are subjects of self-aggregation. The formation of aggregates (micellar mesophases) is energy-favourable (the energy necessary for aggregation of colloidal particles is less than the energy necessary for their dissociation), hence the propensity to structure-forming processes (Hemsley and Griffiths, 2000).

It is generally accepted, following numerous studies on *Arabidopsis* and rice mutants, that sporopollenin monomers are synthesized in the tapetum and then delivered into the developing microspore walls after tetrad disintegration (e.g. Ariizumi *et al.*, 2004; Zhang *et al.*, 2007; Dobritsa *et al.*, 2009, 2011; Grienenberger *et al.*, 2010; Ariizumi and Toriyama, 2011; Lallemand *et al.*, 2013; Liu and Fan, 2013; Lou *et al.*, 2014; Quilichini *et al.*, 2014; Shi *et al.*, 2015; Wang *et al.*, 2018). Interestingly, Wang and coauthors (2018) showed that sporopollenin synthesis genes are highly expressed earlier than generally reported: from the late tetrad stage. Being micelles, the glycocalyx units provide a system for transport of substances derived from the tapetum that are soluble within micelles but insoluble outside them (e.g. sporopollenin precursors and monomers). In some cases not only multiple direct contacts, via strands, between the tapetum and microspores of the dissipating tetrads were shown, but also typical nematic liquid crystals (most probably sporopollenin monomers) were observed in the cytoplasm of the parietal tapetum of *Persea americana* (fig. 5 in Gabarayeva *et al.*, 2010*a*) and the periplasmodial tapetum in *Ambrosia trifida* (fig. 9a, b in Gabarayeva *et al.*, 2018*b*). However, we continue to believe that additional synthesis of sporopollenin monomers could occur in microspores themselves; being low in quantity and difficult to detect, this so-called receptor-dependent sporopollenin (Grigorjeva and Gabarayeva, 2015) accumulates exclusively in the primexine during the tetrad period and is especially resistant to chemical degradation, in contrast with the much greater amounts of receptor-independent, tapetum-derived sporopollenin accumulating in the post-tetrad period (Rowley and Claugher, 1991). Certainly the necessary genes appear to be expressed in both haploid and diploid cells.

Working together (Gabarayeva and Hemsley, 2006; Hemsley and Gabarayeva, 2007), we developed the hypothesis that most of the developmental events during microspore sporoderm development were based on the unfolding sequence of micellar mesophases (Fig. 3 in Hemsley and Gabarayeva, 2007). However, to firmly establish this idea, exine patterns needed to be experimentally simulated. The first experimental efforts to replicate spore wall structures *in vitro* were undertaken by Hemsley and coauthors (Hemsley *et al.*, 1996, 1998, 2003). We followed these modelling experiments using another method and generated structures resembling several separate exine layers (Gabarayeva and Grigorjeva, 2013, 2016, 2017), but did not simulate the widespread columellate ectexine or combined layers of ectexine and endexine.

Our aim in this study was to mimic *in vitro* structures resembling columellate and granulate exines (including lamellate endexine) as seen during the process of development and at maturity.

MATERIALS AND METHODS

Experimental design

The substances used in experiments are represented in Table 1. When selecting the chemical compounds used in the experiments we took into consideration that the contents of the supporting liquid in the periplasmic space changes from hydrophilic to hydrophobic when the lipoid sporopollenin precursors and monomers mentioned above are added into the same volume at the middle tetrad stage. Following our original method (Gabarayeva and Grigorjeva, 2013, 2016), we prepared mixtures of substances, mostly surfactants, naturally occurring in the periplasmic space of the developing microspores or analogous to them (substitutes). The mixtures were then left undisturbed for specific periods of time to allow the process of self-assembly to proceed – in this case condensation by water evaporation. The duration of the experiments was based on the insight that as water from our samples evaporated and condensation proceeded, the emerging patterns became dry and stable, and no further changes occurred. The effect of fixative on these non-living experimental systems is close to that in biological systems, because all the chemical components are organic substances, analogous to those participating in exine development. Small pieces of the resulting dry films were then fixed using conventional methods for transmission electron microscopy (TEM). The mixtures employed, the duration of experiments prior to fixation and the references to figures showing the patterns obtained are summarized in Table 2. In a departure from our previous experiments, we used some new substances, including mucin, lecithin and stearic acid. We also developed a new method of containing some of the mixtures during the condensation process by sandwiching them between two microscope slides, separated by glass capillaries 0.4 mm in diameter (marked in Table 2 with 'T' for thin layer). The other experiments were performed in small Petri dishes using layers 2–3 mm thick. In these experiments, unlike our previous ones (Gabarayeva and Grigorjeva, 2013, 2016), physical constraints were applied to most experimental mixtures (they were placed between microscope slides, separated by glass capillaries) that made the state of colloidal solutions closer to natural conditions of the narrow microspore periplasmic space. The experiments were performed six times with similar results but exhibiting small variations in the size and curvature of structural units.

Fixation and embedding of samples

Small pieces of the dry films obtained after the evaporation of water were fixed in 3 % glutaraldehyde and 2.5 % sucrose in a 0.1 M phosphate buffer (pH 7.3, 20 °C, 24 h), with the addition of 1 % tannic acid (method of fixation adapted from Clark *et al.*, 1983). The material was post-fixed with 2 % osmium tetroxide (pH 8.0, 20 °C, 2 h). After dehydration in an alcohol series, the samples were additionally dehydrated in mixtures of acetone with Epon–Araldite resin, and finally embedded in an Epon–Araldite mixture. Ultrathin sections were stained with a saturated solution of uranyl acetate in ethanol and 0.2% lead citrate. Sections were examined with a Hitachi H-600 transmission electron microscope.

RESULTS

Table 2 presents a brief summary of the results, with the chemical composition of substances used, their concentrations in experimental mixtures, the durations of experiments, and corresponding references to the figures in which the resulting simulation patterns are illustrated.

It can be seen from comparative analysis of patterns in Figs 1 and 2 and data on contents of the mixtures in Table 2 that distinct columellate patterns appeared in those cases where the mixtures included callose and lecithin, and when the process of self-assembly proceeded for a rather long time (10 d) under the constraint of a thin layer. Lecithins, a group of fatty amphiphilic substances, are poorly soluble in water, hence the appearance of hydrophobic and hydrophilic domains in the mixtures (marked by asterisks and stars in Figs 1 and 2, respectively). This means that the columellate-like pattern occurs at the interface between these domains. This pattern corresponds to a typical micellar middle mesophase, with its cylindrical micelles parallel to each other and closely packed in a layer. In some places this pattern appeared as semicircles (Fig. 1A′, B′), in other sites as circles, simulating exine after acetolysis in some species (Fig. 1C′). The developing endexine-like lamellae, with a typical central white line, appeared separately and close under the columellate-like pattern (Fig. 1D′). Slightly different columellate-like patterns simulated natural columellate ectexines seen at the late tetrad stage and at maturity in a number of species (Fig. 2).

Mixture 2, which also contained lecithin, but not callose, and was maintained for a shorter duration (4 d), resulted in the appearance of lamellate patterns, which were string-like (as in Fig. 3A′), resembling the developing endexine in *Ambrosia trifida* (Fig. 3A, A′).

Mixture 3, which lacked callose and lecithin, with different concentrations of the remaining components and with the addition of stearic acid, and with the same duration of the self-assembly process, showed several different patterns. These included developing laminate (= lamellar, neat) micelles with discernible dilations along the laminae (Fig. 3B′), which resembled the primordial endexine lamella in *Michelia fuscata* (Fig. 3B). Such patterns correspond to the peristaltic form of laminate micelles (Fig. 4E in Hemsley and Gabarayeva, 2007), which are capable of self-assembling to the next mesophase – laminate micelles (Fig. 3D′) – simulating the endexine lamellae in *Ambrosia trifida* (Fig. 3D).

Mixture 4 showed separate (Fig. 3C′) and semi-fused laminate micelles, dissipated into spherical micelles at the ends (Fig. 3E′). The latter resembled a margin aperture site in, for example, *Trevesia burckii* (and many other species), where developing endexine lamellae are also fused at the inapertural regions, but are separated at the aperture site (at the oncus, where the periplasmic space is considerable widened) and are dissipated into spherical units inside the free volume of the oncus (Fig. 3E). The difference between two images—3E and 3E′—is that the natural structure in Fig. 3E has accumulated sporopollenin.

Mixture 5 was kept undisturbed for 7 d as a relatively thick layer, so the patterns appeared as a crust on the surface of the samples. The structures observed in these samples represented very typical stacks of laminate micelles, with their gaps between bilayers, seen with TEM as white lines (arrowhead in Fig. 3D″, arrowheads in Fig. 3F′ and arrows in Fig. 4A′). In addition to these stacks, plenty of worm-like micelles (an earlier mesophase of the micellar sequence) were seen (arrowheads in Fig. 4A′). Note the lipid droplets (Fig. 3D″, F′) and lipid domains (Fig. 4A′, white asterisk) associated with stacks of laminate micelles. They make the surrounding medium sufficiently hydrophobic for the self-assembly of laminate micelles, with parallel arrangement, hence the term ‘neat mesophase’. Such micelles compare closely with the young endexine lamellae in all species with laminate endexine, for example in *Anaxagorea brevipes*, until sporopollenin accumulation (Fig. 3F). The image in Fig. 4A′ is very similar to the natural pattern of the *Juniperus communis* free microspore (Fig. 4A). At higher magnification not only were the endexine lamellae evident as typical laminate micelles with white lines, but there were also numerous worm-like micelles crowded in the anther loculus of *Juniperus* (Fig. 4A, arrowhead).

Clusters of parallel laminate micelles with gaps between bilayers (Fig. 4B′), obtained with mixture 6, not only formed the base of the lamellate endexines in microspores, but also appeared in the microspore cytoplasm [e.g. in *Liriodendron chinense* (Fig. 4B) and other Magnoliaceae]. In addition, this mixture was capable of self-assembling a pattern corresponding closely to the mature pollen wall of *Larix decidua* with its granulate ectexine and lamellate endexine (compare Fig. 4C′ and C). Whereas our previous attempt to simulate *Larix* exine resulted in the appearance of two separate mimics – ectexine-like and endexine-like (Gabarayeva and Grigorjeva, 2017) – in this experiment the two layers appeared united. In the magnified fragment shown in Fig. 4C′ the laminate micelles with gaps between them (Fig. 4D′, arrowhead) are especially evident, and it is clear that they form the base for the endexine lamellae (Fig. 4D, E, arrowheads) before sporopollenin accumulates on them.

Mixtures 7 and 8 resulted in the appearance of two-layered mimics (Fig. 5A′, C′, D′, E′), simulating the tetrad spore of extinct *Verrucosisporites narmianus* (Fig. 5A) and pollen walls with more or less structureless (at maturity) ectexine and developing endexine, found in certain Magnoliaceae species (Fig. 5C′, D′, E′; the developing endexine lamellae and their simulations are indicated by arrows or arrowheads). These different types of simulation occur at the interface of the liquid and air phases. A lamellate pattern, as in spores of *Osmundacidites wellmanii* (Fig. 5B, B′), obtained with mixture 2, resembled the lamellated

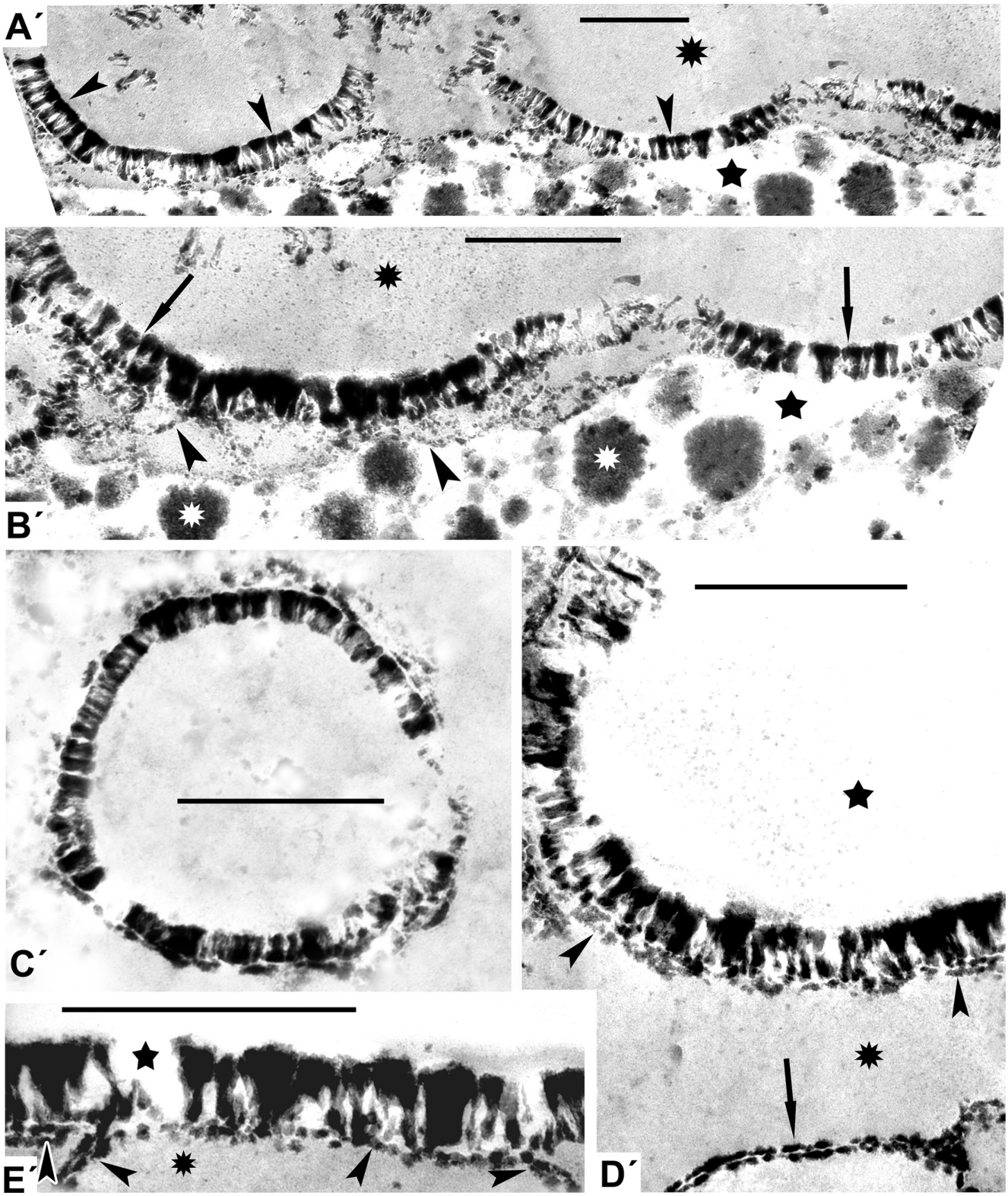

FIG. 1. Models mimicking some developing exines of the tectate–columellate type [in this and other figures, all images marked with a prime (′) are simulations]. (A′) Distinctly columellate pattern (arrowheads corresponds to middle micellar mesophase) in the form of arcs appears at the interface of hydrophobic (asterisk) and hydrophilic (star) domains. (B′) Arcuate patterns with columellate structure (arrows indicate middle mesophase) at the interface of hydrophobic (black asterisk) and hydrophilic (star) domains. The underlying wavy string-like layer (arrowheads) mimics the formation of the foot layer. The aqueous domain contains lipid inclusions (white asterisks). (C′) Ring-shaped columellate pattern mimicking acetolysed tectate–columellate pollen wall. (D′) Simulation of the aqueous/lipid interface mimicking columellate ectexine with developing tectum (arrowheads), and forming a lamella with a central white line (laminate micellae with typical gap; arrow), lying apart. (E′) A pattern simulating the tectate–columellate ectexine pattern with a developing primordial white-lined lamella (arrowheads) at the interface of hydrophobic (asterisk) and hydrophilic (star) domains. Scale bars = 0.5 µm

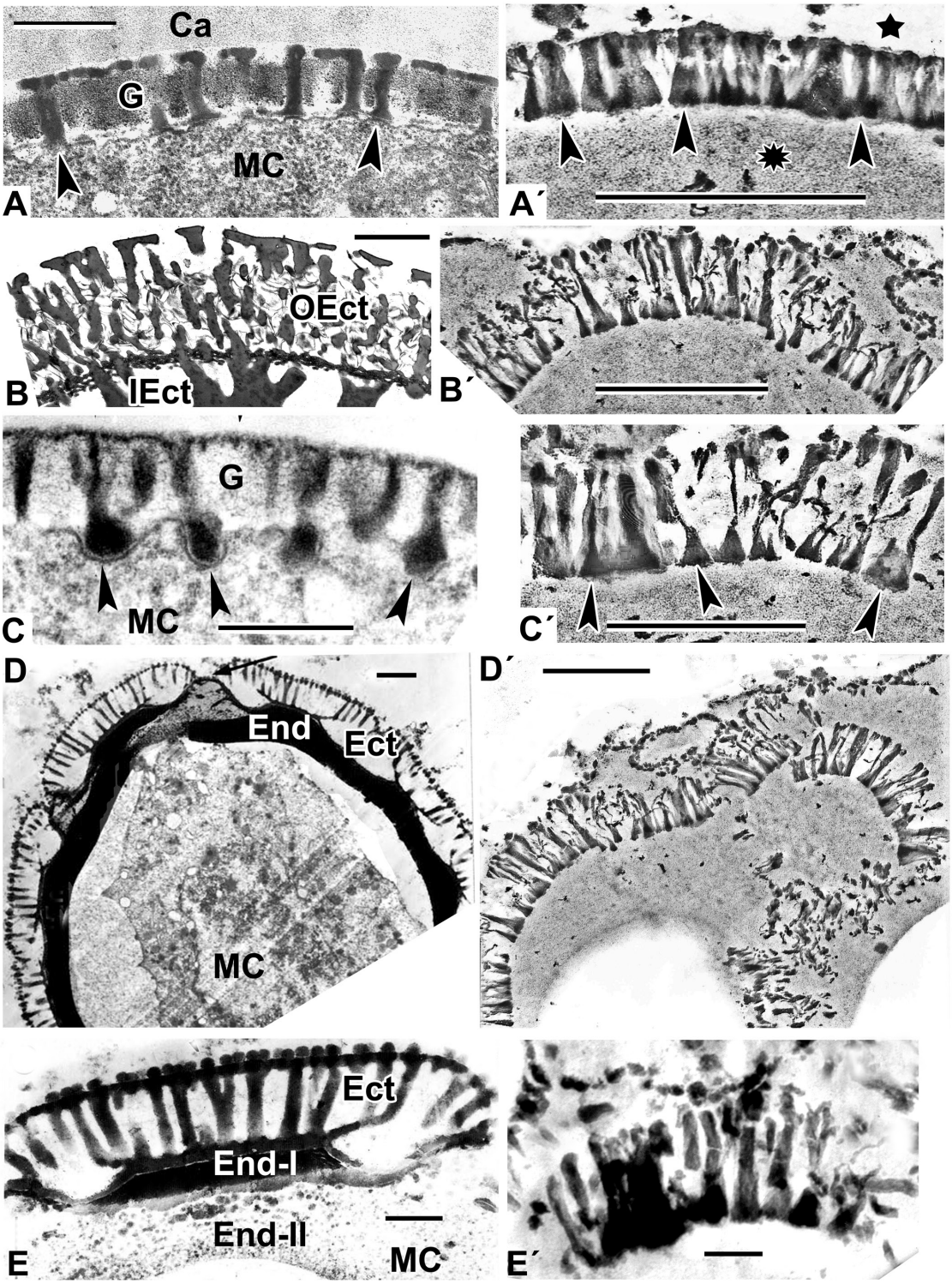

FIG. 2. Natural exine patterns of a number of species (A–E) and experimental patterns simulated by self-assembly (A′–E′). (A) Columellate ectexine in the process of development at the late tetrad stage in *Acer tataricum*. Columellae (arrowheads). (Fig. 4a in Gabarayeva *et al.*, 2010*a*). (A′) Simulation with columellate-like pattern (arrowheads) at the interface between lipidic (asterisk) and aqueous (star) domains. (B) Mature ectexine in *Echinops exaltatus* with outer ectexine (OEct) consisting of thin columellae (united with each other by fine connections) and of inner ectexine (IEct) of thick columellae. (Fig. 11e in Gabarayeva *et al.*, 2018*a*). (B′) Simulation mimicking the outer ectexine in *Echinops*. (C) Late tetrad stage in *Cabomba aquatica*. Developing columellae have widened 'feet' (arrowheads). (Plate III, 9 in Gabarayeva *et al.*, 2003). (C′) Columellae-like simulation; 'columellae' have widened 'feet' (arrowheads). (D) A free microspore of *Borago officinalis* with mature columellate ectexine (Ect) and endexine (End). Aperture site is indicated by an arrow. (Fig. 20 in Rowley *et al.*, 1999). (D′) Simulation partly imitating the ectexine in *Borago*. (E) Magnified interapertural portion of the exine in *Borago officinalis* with columellate ectexine (Ect) and two-layed endexine (End-I and End-II). (Fig. 21 in Rowley *et al.*, 1999). (E′) Simulation similar to partly distorted interapertural ectexine in *Borago*. Scale bars: (A, C, E, A′–D′) = 0.5 μm; (B) = 2 μm; (D) = 1 μm; (E′) = 0.1 μm. Ca, callose; G, glycocalyx; MC, microspore cytoplasm.

pattern shown in Fig. 3B′. The two patterns were related; the second was the next mesophase in comparison with the first.

Another pattern (obtained with mixture 3; Fig. 5F′) was quite different and mimicked the tectate–columellate ectexine in *Chamaedorea microspadix* (Fig. 5F).

A number of fractal structures, typical self-assembling structures (Fig. 6A′–E′), were also obtained from mixture 3. Some of these were similar to natural patterns and could serve as a glycocalyx-like framework (compare Fig. 6A′ and A; the latter is the alveolate exine of *Lepidozamia*). Fractal structures were frequently observed in the anther loculus, for example as pollenkitt deposition with structures like a branched tree in the course of *Symphytum* pollen development (Fig. 6F, G).

DISCUSSION

One important observation resulting from these experiments is that microstructures resembling tectate–columellate ectexine (Figs 1 and 2) arise in the presence of callose, whereas lamellate microstructures, equivalent to endexine (Figs 3 and 4), form when callose is absent. In nature, the same phenomenon takes place: the ectexine appears in the presence of callose, in the tetrad period, but when callose disperses in the free microspore stage the endexine starts to develop. This observation supports the importance of the callosic special cell wall for the establishment of exine patterns, as was suggested previously (Blackmore *et al*., 2007, 2010; Gabarayeva *et al.*, 2018*a*). In our earlier experiments (Gabarayeva and Grigorjeva, 2013, 2016, 2017) we managed to obtain some columellate-like or lamellate-like patterns. However, in this study we generated much more distinct columellate and lamellate patterns, mimicking natural developing and mature ectexines and endexines. We also obtained a simulation of mature exine with combined layers of granulate ectexine and lamellate endexine (Fig. 4C′). Two circumstances explain this result: (1) the wider spectrum of substances in the mixtures, the same as or analogous to those present in pollen development; and (2) carrying out the process of self-assembly in a narrow space between two glass slides. This second feature, which imposes an additional physical constraint, corresponds closely to the narrow periplasmic space between the plasma membrane and the callose special wall that occurs *in vivo*.

TABLE 1. *Comparison of components and their functions for a generalized microsporangium and* in vitro *systems used in experiments*

Substances located inside (or adjacent to) the microspore periplasmic space	Substances of the model systems (natural for a generalized sporangium and substitutes, similar to natural in chemical composition)
Callose (outer boundary layer of microspore tetrads)	Callose (natural) Agar gel (substitute) Hypromellose (substitute)
Glycoproteins and lipopolysaccharides of the glycocalyx (primexine matrix)	Saponin (substitute) Mucin (substitute) Chondroitin (substitute) Lipopolysaccharide (substitute)
Phenolic compounds (sporopollenin monomers)	*p*-Coumaric acid (natural) Vanillic acid (natural)
Unsaturated and saturated aliphatic fatty acids (sporopollenin monomers)	Oleic acid (substitute) Stearic acid (substitute)
Lipid-like surfactants	Lecithin (substitute)
Supporting liquid: water	Water

TABLE 2. *Components and their concentrations and volumes used to produce the structures illustrated in Figs 1A′–C′*

Mixture	Components	DBF	Figures
1	Callose 3 % (aqueous colloidal solution, 2 mL) + hypromellose 3 % (aqueous solution, 2 mL) + mucin 3 % (aqueous solution, 1 mL) + saponin 3 % (aqueous solution, 1 mL) + *p*-coumaric acid 5 % (ethanol solution, 0.5 mL) + lecithin (0.5 mL) + oleic acid (pure, 10 drops*) + vanillic acid (1 % ethanol solution, 10 drops) + stearic acid (1 % ethanol solution, 10 drops)	10T**	1A′–E′, 2A′–E′
2	Chondroitin (1 mL) + hypromellose 3 % (aqueous solution, 2 mL) + mucin 3 % (aqueous solution, 2 mL) + saponin 3 % (aqueous solution, 1 mL) + *p*-coumaric acid 5 % (ethanol solution, 1 mL) + lecithin (0.5 mL) + oleic acid (pure, 3 drops) + vanillic acid (1 % ethanol solution, 8 drops)	4T	3A′, 5B′
3	Chondroitin (1 mL) + hypromellose 3 % (aqueous solution, 1 mL) + mucin 3 % (aqueous solution, 1 mL) + saponin 3 % (aqueous solution, 1 mL) + *p*-coumaric acid 5 % (ethanol solution, 1 mL) + oleic acid (pure, 6 drops) + vanillic acid (1 % ethanol solution, 6 drops) + stearic acid (1 % ethanol solution, 6 drops)	4T	3B′, D′, 5F′, 6A′–E′
4	Hypromellose 3 % (aqueous solution, 2 mL) + mucin 3 % (aqueous solution, 2 mL) + saponin 3 % (aqueous solution, 2 mL) + *p*-coumaric acid 5 % (ethanol solution, 1 mL) + stearic acid (1 % ethanol solution, 1 mL)	4T	3C′, E′
5	Chondroitin (2 mL) + hypromellose 5 % (aqueous solution, 2 mL) + mucin 3 % (aqueous solution, 2 mL) + *p*-coumaric acid 5 % (ethanol solution, 2 mL) + oleic acid (pure, 6 drops) + vanillic acid (1 % ethanol solution, 6 drops)	7	3D″, F′, 4A′
6	Agar 3 % (1 mL, warm solution) + mucin 3 % (aqueous solution, 1 mL) + *p*-coumaric acid (5 % ethanol solution, 1 mL) + saponin 3 % (aqueous solution, 1 mL) + stearic acid (1 % ethanol solution, 1 mL)	4T	4B′–D′
7	Hypromellose 3 % (aqueous solution, 1 mL) + mucin 3 % (aqueous solution, 1 mL) + saponin 3 % (aqueous solution, 1 mL) + *p*-coumaric acid 5 % (ethanol solution, 1 mL) + stearic acid (1 % ethanol solution, 6 drops) + oleic acid (pure, 6 drops) + vanillic acid (1 % ethanol solution, 6 drops)	4	5A′, C′, E′
8	Agar 3 % (2 mL, warm solution) + lipopolysaccharide 2,5 % (2 mL) + *p*-coumaric acid 5 % (ethanol solution, 3 drops) + oleic acid (pure, 3 drops) + vanillic acid (1 % ethanol solution, 3 drops)	2	5D′

*1 drop = 0.04 mL.

**All mixtures marked 'T' were in a thin layer (0.4 mm); others were in layers 2–3 mm thick.

DBF, number of days of self-assembly process before fixation.

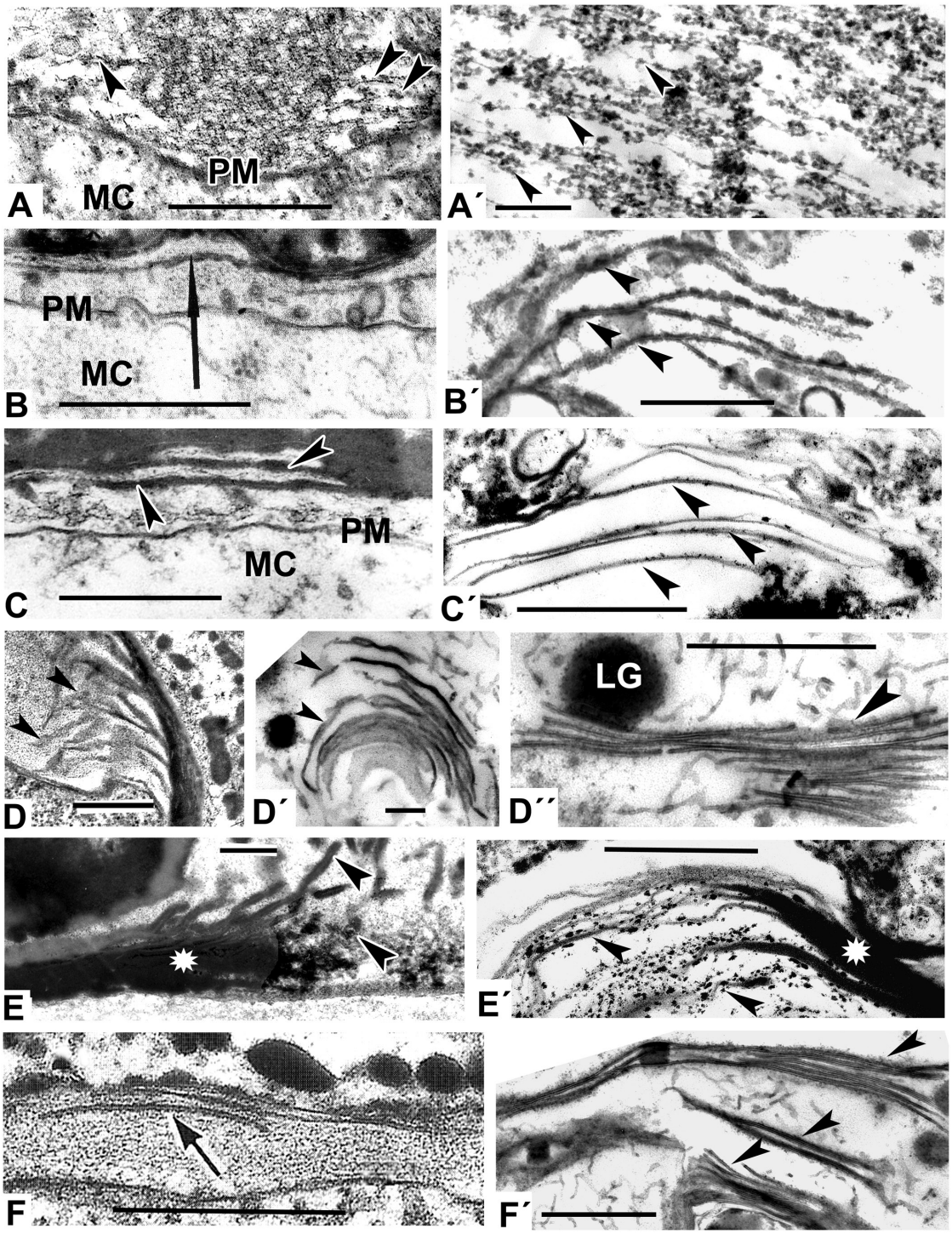

FIG. 3. Models mimicking the developing lamellae of the endexine (A′–F′) comparable with natural patterns (A–F). (A) Initiation of endexine lamellae (arrowheads) at the aperture site of *Ambrosia trifida* microspore. (Fig. 7b in Gabarayeva *et al.*, 2018*b*). (A′) Parallel-oriented strings (one of micellar form, arrowheads) simulating the initial step of endexine lamellae development. (B) Primordial lamella (arrow) of the endexine in *Michelia fuscata* microspore with nodated profile (ectexine is not shown). (Fig. 10B in Gabarayeva and Grigorjeva, 2012). (B′) Model simulating the endexine lamellae in *Michelia fuscata* (peristaltic deformations of laminate mesopase, arrowheads). (C) Endexine lamellae in *Magnolia sieboldii* after sporopollenin accumulation (arrowheads; the ectexine is not shown). (Fig. 12A in Gabarayeva and Grigorjeva, 2012). (C′) Laminate micelles (arrowheads) simulating the endexine lamellae before sporopollenin accumulation. (D) Endexine lamellae (arrowheads) at the aperture site of *Ambrosia trifida* microspore. (Fig. 11e in Gabarayeva *et al.*, 2018*b*). (D′) Laminate micelles of a model (arrowheads) simulating the endexine lamellae in *Ambrosia trifida*. (D″) Stack of typical laminate micelles (arrowhead) simulating the endexine lamellae in many species with typical central white lines. (E) An aperture site in *Trevesia burckii* with the endexine lamellae compressed at the margin of the aperture (asterisk) but separated from each other and dissipated into spherical units at the ends at the apertural site (arrowheads; the ectexine is not shown). (Plate IV, 5 in Gabarayeva *et al*., 2009). (E′) Simulation mimicking the endexine at the margin of aperture site in *Trevesia burckii*: fused laminate micelles (asterisk), partly dissipated into spherical micelles (arrowheads). (F) Endexine lamellae in *Anaxagorea brevipes* (arrow). (F′) Simulation mimicking the endexine lamellae (arrowheads) in *Anaxagorea brevipes*. LG, lipid globule; MC, microspore cytoplasm; PM, plasma membrane. Scale bars = 0.5 µm

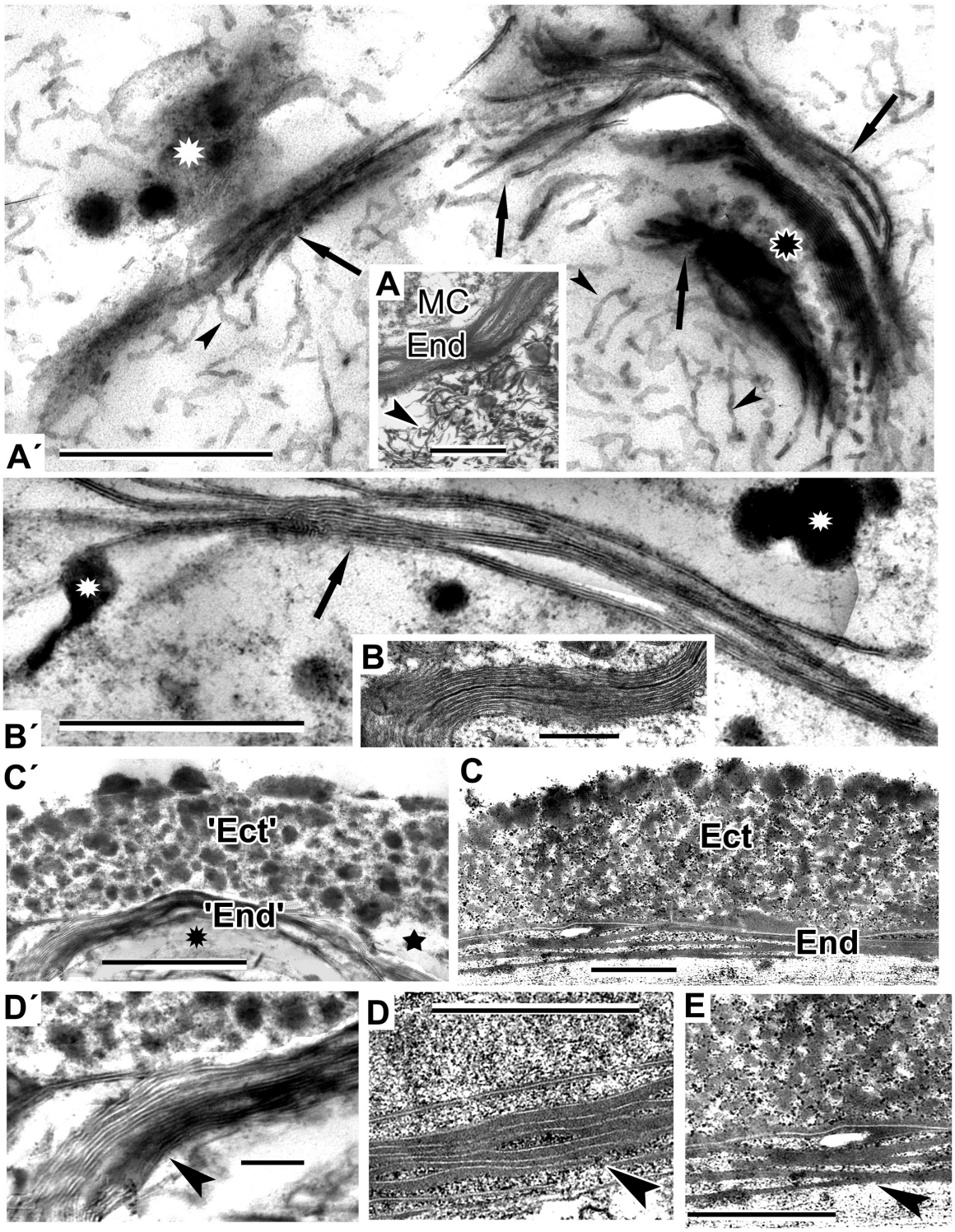

FIG. 4. The process of gradual experimental micellar self-assembly resulting in the arrangement of an exine-like pattern in *Larix decidua*. (A′) Numerous wavy, worm-like micelles (arrowheads), which self-aggregate into clusters (arrows) where lipid droplets are located (white asterisk). Note the area of spherical micelles (black asterisk). (A) Fragment of a *Juniperus communis* free microspore with lamellate endexine (End). Note numerous worm-like micelles in the anther loculus (arrowhead). (B′) Advanced stage of self-assembly. Typical laminate micelles, where dark-contrasted layers alternate with 'white lines', simulating the endexine lamellae. (B) Laminate micelles not only form the base of endexine lamellae, but also occur in the microspore cytoplasm, e.g. in microspores of *Liriodendoron chinense*. (C′) More advanced stage of self-assembly: a pattern simulating granular ectexine ('Ect') and lamellate endexine ('End') in *Larix decidua* at the interface between hydrophilic (star) and hydrophobic (asterisk) domains. (C) Exine of *Larix decidua* with granulate ectexine (Ect) and lamellate endexine (End). (D′) Magnification of part of C′ to show a stack of laminate micelles with gaps between them (arrowhead). Note less (left) and more (right) compressed portions of the micelle stack. (D, E) Endexine in *Larix* at higher magnification: more (D) and less (E) compressed lamellae (arrowheads). (D, E are parts of Figs 8c and 11a in Gabarayeva and Grigorjeva, 2017). Scale bars: (D′) = 0.1 µm; (all others) = 0.5 µm. MC, microspore cytoplasm.

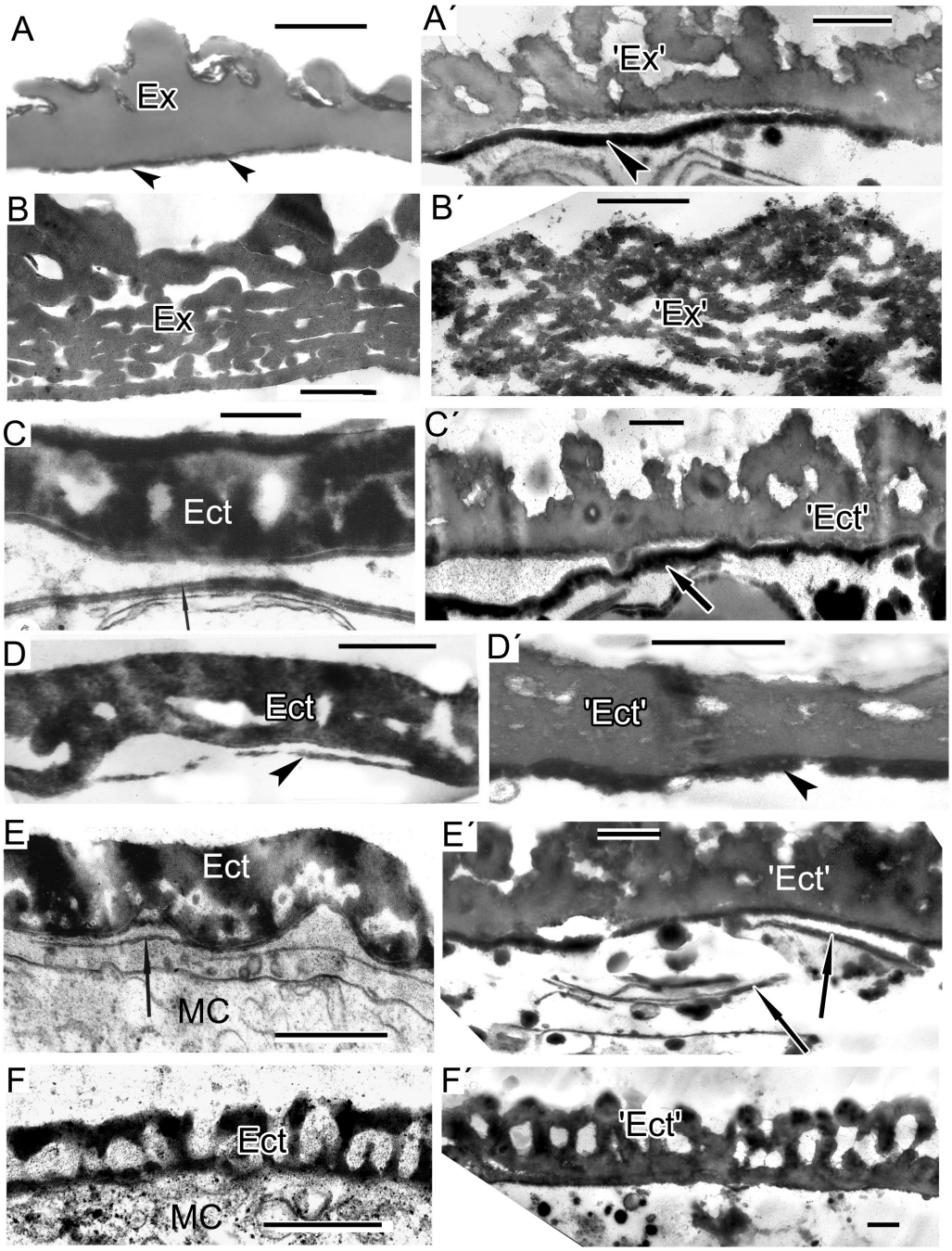

FIG. 5. Spore and exine patterns of a number of species (A–F) and experimental patterns simulating them by self-assembly (A′–F′). (A, B) Megaspore walls of extinct representatives of the genera *Verrucosisporites* and *Osmundacidites*: *Verrucosisporites narmianus* (A) and *Osmundacidites wellmanii* (B) (courtesy of V. Tarasevich) and simulations mimicking them (A′, B′). The dark contrast layer in A′ (arrowhead) mimics a probable endospore layer in A (arrowheads). (C) Microspore wall in *Magnolia delavayi* with ectexine (Ect) and developing endexine (arrow). (Fig. 10A in Gabarayeva and Grigorjeva, 2012). (C′) Model simulating the ectexine and endexine (arrow) of *Magnolia* microspore wall. (D) Acetolysed pollen wall in *Magnolia delavayi*, with the endexine indicated by an arrowhead. (Fig. 14E in Gabarayeva and Grigorjeva, 2012). (D′) Simulation resembling the acetolysed pollen wall in *Magnolia delavayi*. (E) Microspore wall of *Michelia fuscata* with the ectexine (Ect) and the developing lamellae of the endexine (arrow). (Fig. 10B in Gabarayeva and Grigorjeva, 2012). (E′) Simulation of *Michelia* microspore wall mimicking ectexine ('Ect') and the developing lamellae of the endexine (arrows). (F) Ectexine in *Chamaedorea microspadix*. (Fig. 7a in Gabarayeva and Grigorjeva, 2010). (F′) Simulation mimicking the ectexine of *Chamaedorea*. Scale bars: (A, B) = 1 µm; (C–F, A′–F′) = 0.5 µm. Ex, exosporium; MC, microspore cytoplasm.

Another important point is that the columella-like pattern occurs *at the interface* between the hydrophilic and hydrophobic domains. The phenomenon of self-assembly activity at interfaces is a regular feature of micellar systems, incorporating surface-active substances. The columella-like pattern is represented by the middle (hexagonal) micellar mesophase, in

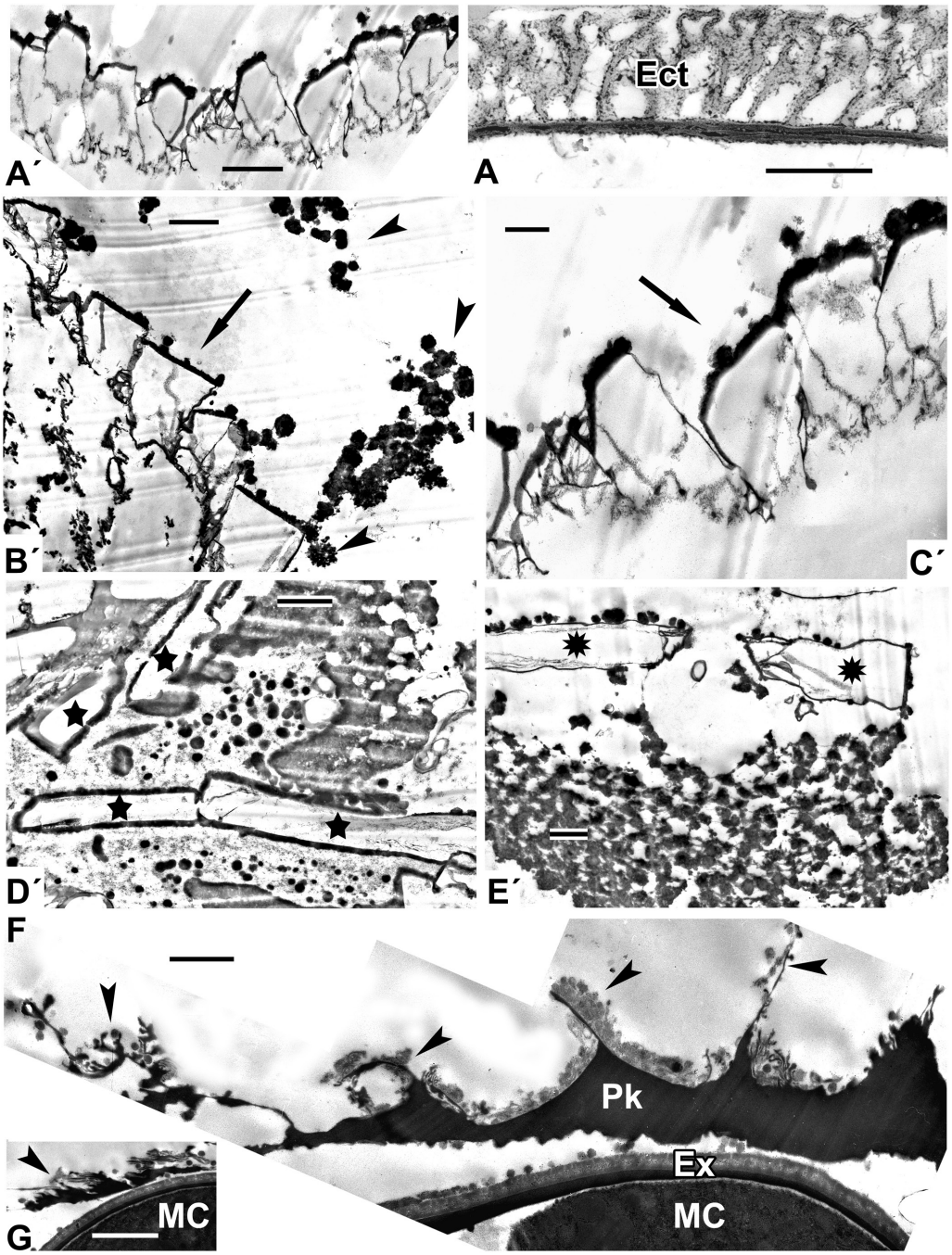

FIG. 6. Fractal (self-similar) patterns, self-assembling in experiments (A′–E′) and in nature (F, G). (A′) One of the fractal structures, simulating the alveolate pattern of the exine in *Lepidozamia* sp. (A). (B′, C′) Two sequences of fractal units (arrows), surrounded by spherical micelles (arrowheads). (D′, E′) Another type of fractal unit, resembling bricks (D′, stars) and flags (E′, asterisks). (F, G) Pollenkitt deposition inside the anther loculus in *Symphytum officinale*, located around microspores, with complex branching structures on the surface; typical fractal structures (arrowheads). (Parts of Fig. 11c in Gabarayeva *et al.*, 2011*b*). Scale bars = 1 µm. Ect, ectexine; Ex, exine; G, glycocalyx; MC, microspore cytoplasm; Pk, pollenkitt.

which numerous parallel cylindrical micelles are tightly packed together in a layer. Evidently, the same processes occur in the natural environment of the periplasmic space of developing microspores. It should be emphasized that the geometrically regular pattern of middle mesophase is typical of inorganic surfactant systems, but in organic systems micelles of any mesophase are slightly distorted; for example, the micelles in Figs 1 and 2 look bone-like rather than cylinder-like.

Some mixtures gave rise to different patterns at different locations of the sample. The appearance of these different structures can be explained by non-uniformity of the mixtures and the formation of hydrophilic and hydrophobic domains after the period in which there was no disturbance.

In contrast to columella-like patterns arising at the interfaces, lamellate patterns simulating white-lined stacks of endexine lamellae occurred *inside* the hydrophobic domains, associated

with lipid droplets (Figs 3 and 4). This can also be observed in Fig. 1B′, D′ and E′, where lamellate structures with central white lines, simulating the developing primordial endexine lamella, underlie the columellate-like pattern, being located within hydrophobic domains. Once again, this is a regular consequence of micellar self-assembling systems, where an advanced mesophase with neat, or laminate, micelles appears when the concentration of surfactants is sufficiently high. First, worm-like micelles fill in the domains, then single laminate micelles and finally stacks of laminate micelles with their typical regular gaps between bilayers (neat mesophases) mimic the process of endexine development in species with this type of endexine, characterized by stacks of lamellae with the well-known 'central white lines' observed by TEM.

Micellar systems in general, especially heterogeneous ones such as those seen in these experiments, are unstable and easily shift from one mesophase to another in both directions. This explains the coexistence of different types of micelle at a given location. Forms such as giant supra-spherical micelles can coexist with laminate micelles, eventually forming the whole layer, mimicking the granulate ectexine in *Larix* (Fig. 4C′). In our experiment, such coexistence was possible on the interface of hydrophilic and hydrophobic domains of the mixture. In the medium of the *Larix* periplasmic space, early sporopollenin accumulation on spherical micelles stops the sequence of mesophase, preventing further transition of spherical to cylindrical micelles and giving rise mainly to granules, with rarely columella-like units.

Simulations on the surface of samples at the interface between colloidal solutions and the air, where less or no constraints of pressure are imposed on the sample surface, mainly show characters of some spore and basal angiosperms walls, where many features are ancestral (Fig. 5). These simulations mimic mainly massive, almost structureless ectexines, and the endexine consisting of a few lamellae, as has been observed in an ontogenetic study in some Magnoliaceae species (Gabarayeva and Grigorjeva, 2012). It should be noted that in nature endexine lamellae, in contrast to ectexines, arise directly from laminate micelles, without the involvement of the glycocalyx. This could be significant in that layers, laminae and white-lined lamellae of spores originated earlier in evolution, using this simpler process of development. Another reason why most spores have walls mainly consisting of white-lined lamellae and lack elaborate sporoderms is the absence of callose in these groups of plants (see review table in Gabarayeva and Hemsley, 2006). It is callose, together with the plasma membrane, that imposes the necessary constraints on the medium in the periplasmic space, promoting the self-assembly processes.

It is worth noting that the pattern of tectate–columellate ectexine in *Chamaedorea* (Fig. 5F) does not differ significantly from the pattern of the alveolate ectexine in *Lepidozamia* (Fig. 6A), and both could be derived from the *in vitro* structures shown in Fig. 5F′. Once again, this shows that there are no abrupt boundaries between exine types and one type can be easily transformed into another. However, in nature the developmental pathways do differ between species. The important question is, in what way does development differ between taxa? There can be significant differences in the relative timing, quantities and precise chemical composition of the material synthesized, or the pH of the supporting medium in the periplasmic space. All of these are assumed to be the genetically controlled components of development. The same underlying processes can give rise to different types of exine. The nature of the underlying mechanisms, being fundamentally similar, is capable of constructing different morphologies by means of variations in such parameters as concentrations of solutions, pH and spatial constraints.

It is interesting to compare our hypothesis on exine development with others. J. Rowley made many detailed studies of ectexine and endexine substructure, development and function (see the full list of papers in Blackmore and Skvarla, 2012). The glycocalyx consists of radial units, ultimately forming a cylindrical structure, described by Rowley as 'tufts' and represented as the fundamental units of ectexines (Rowley and Flynn, 1968; Rowley *et al.*, 1981; Rowley, 1990). We agree with this and consider that Rowley's tufts correspond to individual cylindrical micelles or clusters of them (Gabarayeva and Hemsley, 2006 and all papers published by our group subsequently). Lamellated endexines with white-line-centred laminae (WLCL), have long been recognized as a fundamental component of spore and pollen grain walls. Rowley's interpretation (Rowley, 1987–1988) of the substructure of endexine (based on the example of *Epilobium*) was that the endexine consisted of short tufts, connected to either side of the WLCL, and that white lines were junction planes between groups of tufts. We suggest that these short tufts in endexine of *Epilobium* could be a row of cylindrical micelles – the middle mesophase (after sporopollenin accumulation). However, it is now evident that white-line-centred lamellae are 'neat' (lamellar) micelles, separated by a layer of water – a liquid crystal mesophase. It is highly probable that in the case of *Epilobium* the endexine appears as the alternation of the two mesophases (middle and lamellar) in the course of phase transition.

It was recently confirmed mathematically that a physical process could drive pattern formation and that the observed diversity of patterns could be explained by viewing pollen pattern development as a phase transition to a spatially modulated phase (Lavrentovich *et al.*, 2016). Moreover, these authors, in their forthcoming paper (Radja *et al.*, 2019) have shown experimentally that phase separation of the extracellular polysaccharide material (primexine) during pollen cell development leads to a spatially modulated phase, and that most of the pollen micro-patterns observed in biological evolution could result from a physical process of modulated phases. These findings are similar to and support our interpretations, and, together with our mimicking experiments, confirm our self-assembly hypothesis.

These results should inform the direction of future molecular genetic studies of pollen wall development. More than 100 genes have been reported as playing a role in exine deposition (Ariizumi and Toriyama, 2011; Dobritsa *et al.*, 2011; Shi *et al.*, 2015) but there has so far been little success in distinguishing which gene products fine-tune the colloidal environment, which provide sporopollenin precursors and which regulate the relative timing of development. Given the apparently universal importance of self-assembly in nature (Lintilhac, 2014; Sampathkumar *et al.*, 2014), a great challenge for the future is to better understand how the interplay of genes establishes subtly different arenas in which physico-chemical processes create ultrastructural and morphological diversity.

Our results have direct relevance to discussions on the origin of angiosperms. Many discussions have focused on whether the earliest angiosperms had tectate–columellate or granular ectexine. The near-basal phylogenetic position of Nymphaeales (Soltis *et al.*, 2005; Chanderbali *et al.*, 2016) implied that their columellate exine was most primitive. However, our results show that while these two morphologies appear rather different, they share the same underlying developmental mechanism of self-assembly. Furthermore, because micellar systems exhibit a non-equilibrium state, mesophases are often mixed (resulting e.g. in both columellate and granulate regions in the *Nymphaeae colorata* exine; Gabarayeva and Rowley, 1994). Similar observations were made on basal angiosperms (Taylor and Osborn, 2006), so that Doyle and Endress (2000), in addition to granular and columellar states, recognized an 'intermediate' state for the infratectum. Taylor and Osborn (2006) agreed that recognizing an intermediate state was a prudent step, and the authors emphasized (Taylor *et al.*, 2015) that variation in pollen characters within Nymphaeales indicated significant potential for lability in pollen development. These observations are strongly supported by our experimental work on micellar self-assembly. Given that spherical micelles serve as the starting point of both granular and columellate ectexines, it is clear that these morphologies are two outcomes of the same process and could not be used to distinguish angiosperms from non-angiosperms in the fossil record.

Conclusions

Our results show how simple physical–chemical interactions are capable of generating typical exine-like patterns, mainly at the interfaces of hydrophilic and hydrophobic domains of colloidal mixtures. This provides compelling evidence that both the genome and self-assembly share control of exine formation. The genome determines chemical compositions, concentrations and the relative timing according to which substances are delivered into the periplasmic space. In its turn, self-assembly takes colloidal micellar systems through the sequence of phase transitions of micellar mesophases and creates a pattern that is finally fixed by accumulation of the biopolymer sporopollenin. It is increasingly apparent that self-assembly processes modify the working of the genome. Given that self-organizing processes are highly energy-efficient, it is perhaps not surprising that they occur in so many biological settings. Biophysically integrated control processes provide an independent, non-genetic context for understanding plant morphogenesis, confirming the opinion of Mandelbrot (1982) that nature need not overload genetic code with detail that is predetermined by self-assembly.

ACKNOWLEDGEMENTS

This work was supported by Russian Foundation for Basic Research grant 17-04-00517*a* to N.G. The Foundation number is 501100002261. The work was carried out in the framework of the institutional research project of the Komarov Botanical Institute of the Russian Academy of Sciences 'Morphology, ultrastructure and development of sporoderm in higher plants' (no. AAAA-A18-118032190134-3) using the equipment of the Core Facility 'Cellular and Molecular Technologies in Plant Science' of the Komarov Botanical Institute (St Petersburg). Special thanks to Stephen Blackmore for advice and help in the course of preparation of the manuscript. N.I.G. designed and performed the experiments, took TEM pictures, performed the principal analysis and wrote the article. V.V.G. fixed and embedded the samples and prepared ultrathin sections. A.L.S. provided consultation in the field of chemistry and technical support. The authors declare no competing interests.

LITERATURE CITED

Ariizumi T, Toriyama K. 2011. Genetic regulation of sporopollenin synthesis and pollen exine development. *Annual Review of Plant Biology* **62**: 1–24.

Ariizumi T, Hatakeyama K, Hinata K, *et al.* 2004. Disruption of the novel plant protein NEF1 affects lipid accumulation in the plastids of the tapetum and exine formation of pollen, resulting in male sterility in *Arabidopsis thaliana*. *Plant Journal* **39**: 170–181.

Benítez M. 2013. An interdisciplinary view on dynamic models for plant genetics and morphogenesis: scope, examples and emerging research avenues. *Frontiers in Plant Science* **4**: 7.

Blackmore S, Skvarla J. 2012. John Rowley (1926–2010), palynologist extraordinaire. *Grana* **51**: 77–83.

Blackmore S, Wortley AH, Skvarla JJ, Rowley JR. 2007. Pollen wall development in flowering plants. *New Phytologist* **174**: 483–498.

Blackmore S, Wortley AH, Skvarla JJ, Gabarayeva NI, Rowley JR. 2010. Developmental origins of structural diversity in pollen walls of Compositae. *Plant Systematics and Evolution* **284**: 17–32.

Chanderbali AS, Berger BA, Howarth DG, Soltis PS, Soltis DE. 2016. Evolving ideas on the origin and evolution of flowers: new perspectives in the genomic era. *Genetics* **202**: 1255–1265.

Clark AH, Richardson RK, Ross-Murphy SB, Stubbs JM. 1983. Structural and mechanical properties of agar/gelatin co-gels. *Marcomolecules* **16**: 1367–1374.

Collinson ME, Hemsley AR, Taylor WA. 1993. Sporopollenin exhibiting colloidal organization in spore walls. *Grana Supplement* **1**: 31–39.

Dickinson HG, Sheldon JM. 1986. The generation of patterning at the plasma membrane of the young microspore of *Lilium.* In: Blackmore S, Ferguson IK, eds. *Pollen and spores: form and function.* London: Academic Press, 1–18.

Dobritsa AA, Shrestha J, Morant M, *et al.* 2009. CYP704B1 Is a long-chain fatty acid ω-hydroxylase essential for sporopollenin synthesis in pollen of *Arabidopsis*. *Plant Physiology* **151**: 574–589.

Dobritsa AA, Geanconteri A, Shrestha J, *et al.* 2011. A large-scale genetic screen in *Arabidopsis* to identify genes involved in pollen exine production. *Plant Physiology* **157**: 947–970.

Doyle JA, Endress PK. 2000. Morphological phylogenetic analysis of basal angiosperms: comparison and combination with molecular data. *International Journal of Plant Sciences* **161**(6, Supplement): S121–S153.

Gabarayeva NI. 1990. Hypothetical ways of exine structure determination. *Botanicheskii Zhurnal* **75**: 1353–1362 (in Russian with English abstract).

Gabarayeva NI. 1991. Patterns of development in primitive angiosperm pollen. In: Blackmore S, Barnes SH, eds. *Pollen spores: patterns of diversification.* Oxford: Clarendon Press, 257–268.

Gabarayeva NI. 1993. Hypothetical ways of exine pattern determination. *Grana* **33** Supplement 2: 54–59.

Gabarayeva NI. 2014. Role of genetic control and self-assembly in gametophyte sporoderm ontogeny: hypotheses and experiment. *Russian Journal of Developmental Biology* **45**: 177–195.

Gabarayeva NI, Grigorjeva VV. 2010. Sporoderm ontogeny in *Chamaedorea microspadix* (Arecaceae). Self-assembly as the underlying cause of development. *Grana* **49**: 91–114.

Gabarayeva NI, Grigorjeva VV. 2011. Sporoderm development in *Swida alba* (Cornaceae), interpreted as a self-assembling colloidal system. *Grana* **50**: 81–101.

Gabarayeva N, Grigorjeva V. 2012. Sporoderm development and substructure in *Magnolia sieboldii* and other Magnoliaceae: an interpretation. *Grana* **51**: 119–147.

Gabarayeva NI, Grigorjeva VV. 2013. Experimental modelling of exine-like structures. *Grana* **52**: 241–257.

Gabarayeva NI, Grigorjeva VV. 2014. Sporoderm and tapetum development in *Eupomatia laurina* (Eupomatiaceae). An interpretation. *Protoplasma* **251**: 1321–1345.

Gabarayeva N, Grigorjeva V. 2016. Simulation of exine patterns by self-assembly. *Plant Systematics and Evolution* **302**: 1135–1156.

Gabarayeva NI, Grigorjeva VV. 2017. Self-assembly as the underlying mechanism for exine development in *Larix decidua* D. C. *Planta* **246**: 471–493.

Gabarayeva NI, Hemsley AR. 2006. Merging concepts: the role of self-assembly in the development of pollen wall structure. *Review of Palaeobotany and Palynology* **138**: 121–139.

Gabarayeva NI, Rowley JR. 1994. Exine development in *Nymphaea colorata* (Nymphaeaceae). *Nordic Journal of Botany* **14**: 671–691.

Gabarayeva NI, Grigorjeva VV, Rowley JR. 2003. Sporoderm ontogeny in *Cabomba aquatica* (Cabombaceae). *Review of Palaeobotany and Palynology* **127**: 147–173.

Gabarayeva NI, Grigorjeva VV, Rowley JR, Hemsley AR. 2009*a*. Sporoderm development in *Trevesia burckii* (Araliaceae). I. Tetrad period: further evidence for the participation of self-assembly processes. *Review of Palaeobotany and Palynology* **156**: 233–247.

Gabarayeva NI, Grigorjeva VV, Rowley JR. 2010*a*. Sporoderm development in *Acer tataricum* (Aceraceae). An interpretation. *Protoplasma* **247**: 65–81.

Gabarayeva NI, Grigorjeva VV, Rowley JR. 2010*b*. A new look at sporoderm ontogeny in *Persea americana*. Micelles and the hidden side of development. *Annals of Botany* **105**: 939–955.

Gabarayeva NI, Grigorjeva VV, Marquez G. 2011*a*. Ultrastructure and development during meiosis and the tetrad period of sporogenesis in the leptosporangiate fern *Alsophila setosa* (Cyatheaceae) compared with corresponding stages in *Psilotum nudum* (Psilotaceae). *Grana* **50**: 235–262.

Gabarayeva N, Grigorjeva V, Polevova S. 2011*b*. Exine and tapetum development in *Symphytum officinale* (Boraginaceae). Exine substructure and its interpretation. *Plant Systematics and Evolution* **296**: 101–120.

Gabarayeva NI, Grigorjeva VV, Kosenko J. 2013. I. Primexine development in *Passiflora racemosa* Brot. Overlooked aspects of development. *Plant Systematics and Evolution* **299**: 1013–1035.

Gabarayeva NI, Grigorjeva VV, Blackmore S. 2016. Pollen wall substructure and development in *Tanacetum vulgare* (Compositae: Anthemideae): revisiting hypotheses on pattern formation in complex cell walls. *International Journal of Plant Sciences* **177**: 347–370.

Gabarayeva N, Grigorjeva V, Polevova S, Hemsley AR. 2017. Pollen wall and tapetum development in *Plantago major* (Plantaginaceae): assisting self-assembly. *Grana* **56**: 81–111.

Gabarayeva NI, Polevova SV, Grigorjeva VV, Blackmore S. 2018*a*. Assembling the thickest plant cell wall: exine development in *Echinops* (Asteraceae, Cynareae). *Planta* **248**: 323–346.

Gabarayeva NI, Polevova SV, Grigorjeva VV, Severova EE, Volkova OA, Blackmore S. 2018*b*. Suggested mechanisms underlying pollen wall development in *Ambrosia trifida* (Asteraceae: Heliantheae). *Protoplasma* doi:10.1007/s00709-018-1320-3.

Gerasimova-Navashina EN. 1973. Physico-chemical nature of primexine formation of angiosperm pollen grains. In: Kovarski A, ed. *Embryology of angiosperms*. Kishinev: Ştiinţă, 57–70.

Grienenberger E, Kim SS, Lallemand B, *et al.* 2010. Analysis of TETRAKETIDE α-PYRONE REDUCTASE function in *Arabidopsis thaliana* reveals a previously unknown, but conserved, biochemical pathway in sporopollenin monomer biosynthesis. *Plant Cell* **22**: 4067–4083.

Grigorjeva V, Gabarayeva N. 2015. The development of sporoderm, tapetum and Ubisch bodies in *Dianthus deltoides* (Caryophyllaceae): self-assembly in action. *Review of Palaeobotany and Palynology* **219**: 1–27.

Gubatz S, Wiermann R. 1992. Studies on sporopollenin biosynthesis in *Tulipa* anthers. 3. Incorporation of specifically labeled C-14 phenylalanine in comparison to other precursors. *Botanica Acta* **105**: 407–413.

Gubatz S, Herminghaus S, Meurer B, Strack D, Wiermann R. 1986. The location of hydroxycinnamic acid amides in the exine of *Corylus* pollen. *Pollen and Spores* **28**: 347–354.

Hemsley AR, Gabarayeva NI. 2007. Exine development: the importance of looking through a colloid chemistry "window". *Plant Systematics and Evolution* **263**: 25–49.

Hemsley AR, Griffiths PC. 2000. Architecture in the microcosm: biocolloids, self-assembly and pattern formation. *Philosophical Transactions of the Royal Society of London A* **358**: 547–564.

Hemsley AR, Collinson ME, Brain APR. 1992. Colloidal crystal-like structure of sporopollenin in the megaspore walls of recent *Selaginella* and similar fossil spores. *Botanical Journal of the Linnean Society* **108**: 307–320.

Hemsley AR, Collinson ME, Kovach WL, Vincent B, Williams T. 1994. The role of self-assembly in biological systems: evidence from iridescent colloidal sporopollenin in *Selaginella* megaspore walls. *Philosophical Transactions of the Royal Society of London B* **345**: 163–173.

Hemsley AR, Jenkins PD, Collinson ME, Vincent B. 1996. Experimental modelling of exine self-assembly. *Botanical Journal of the Linnean Society* **121**: 177–187.

Hemsley AR, Vincent B, Collinson ME, Griffiths PC. 1998. Simulated self-assembly of spore exines. *Annals of Botany* **82**: 105–109.

Hemsley AR, Griffiths PC, Mathias R, Moore SEM. 2003. A model for the role of surfactants in the assembly of exine sculpture. *Grana* **42**: 38–42.

Heslop-Harrison J. 1972. Pattern in plant cell walls: morphogenesis in miniature. *Proceedings of the Royal Institution of Great Britain* **45**: 335–351.

Ingber D. 1993. Cellular tensegrity: defining new rules of biological design that govern the cytoskeleton. *Journal of Cell Sciences* **104**: 613–627.

Kauffman SA. 1993. *The origin of order.* New York: Oxford University Press.

Kurakin A. 2005. Self-organization versus watchmaker: stochastic dynamics of cellular organization. *Biological Chemistry* **386**: 247–254.

Lallemand B, Erhardt M, Heitz T, Legrand M. 2013. Sporopollenin biosynthetic enzymes interact and constitute a metabolon localized to the endoplasmic reticulum of tapetum cells. *Plant Physiology* **162**: 616–625.

Lavrentovich MO, Horsley EM, Radja A, Sweeney AM, Kamien RD. 2016. First-order patterning transitions on a sphere as a route to cell morphology. *Proceedings of the National Academy of Sciences of the USA* **113**: 5189–5194.

de Leeuw JW, Versteegh GJM, van Bergen PF. 2006. Biomacromolecules of algae and plants and their fossil analogues. *Plant Ecology* **182**: 209–233.

Legrand M. 2010. Analysis of tetraketide α-pyrone reductase function in *Arabidopsis thaliana* reveals a previously unknown, but conserved, biochemical pathway in sporopollenin monomer biosynthesis. *Plant Cell* **22**: 4067–4083.

Li FS, Phyo P, Jacobowitz J, Hong M, Weng J-K. 2019. The molecular structure of plant sporopollenin. *Nature Plants* **5**: 41–46.

Lintilhac PM. 2014. The problem of morphogenesis: unscripted biophysical control systems in plants. *Protoplasma* **251**: 25–36.

Liu L, Fan X-D. 2013. Tapetum: regulation and role in SP biosynthesis in *Arabidopsis*. *Plant Molecular Biology* **83**: 165–175.

Lou Y, Xu XF, Zhu J, Gu JN, Blackmore S, Yang ZN. 2014. The tapetal AHL family protein TEK determines nexine formation in the pollen wall. *Nature Plants* doi:10.1038/ncomms4855.

Mandelbrot BB. 1982. *The fractal geometry of nature*. San Francisco: W. H. Freeman.

Niester-Nyveld C, Haubrich A, Kampendonk H, *et al.* 1997. Immunocytochemical localization of phenolic compounds in pollen walls using antibodies against *p*-coumaric acid coupled to bovine serum albumin. *Protoplasma* **197**: 148–159.

Pettitt JM. 1979. Ultrastructure and cytochemistry of spore wall morphogenesis. In: Dyer AF, ed. *The experimental biology of ferns*. London: Academic Press, 211–252.

Pettitt JM, Jermy AC. 1974. The surface coats on spores. *Botanical Journal of the Linnean Society* **6**: 245–257.

Quilichini TD, Douglas CJ, Samuels AL. 2014. New views of tapetum ultrastructure and pollen exine development in *Arabidopsis thaliana*. *Annals of Botany* **114**:1189–1201.

Quilichini TD, Grienenberger E, Douglas CJ. 2015. The biosynthesis, composition and assembly of the outer pollen wall: a tough case to crack. *Phytochemistry* **113**: 170–182.

Radja A, Horsley EM, Lavrentovich MO, Sweeney AM. 2019. Pollen patterns form from modulated phases. *Cell* **176**: 856–868..

Rowley JR. 1971. Implications on the nature of sporopollenin based upon pollen development. In: Brooks J, Grant PR, Muir M, van Gijzel P, Shaw G, eds. *Sporopollenin*. London: Academic Press, 174–219.

Rowley JR. 1975. Lipopolysaccharide embedded within the exine of pollen grains. In: Bailey GW, ed. *33rd Annual Proceedings of the Electron Microscopy Society of America, Las Vegas, NV*, 572–573.

Rowley JR. 1987–1988. Substructure within the endexine, an interpretation. *Journal of Palynology*, **23/24**: 29–42.

Rowley JR. 1990. The fundamental structure of the pollen exine. *Plant Syst Evol* **suppl 5**: 13–29.

Rowley JR, Claugher D. 1991. Receptor-independent sporopollenin. *Botanica Acta* **104**: 316–323.

Rowley JR, Dahl AO. 1977. Pollen development in *Artemisia vulgaris* with special reference to glycocalyx material. *Pollen and Spores* **19**: 169–284.

Rowley JR, Dahl AO, Sengupta S, Rowley JS. 1981. A model of exine substructure based on dissection of pollen and spore exines. *Palynology* **5**: 107–152.

Rowley JR, Flynn JJ. 1968. Tubular fibrils and the ontogeny of the yellow water lily pollen grain. *Cell Biology* **39**: 159.

Rowley JR, Skvarla JJ, Gabarayeva NI. 1999. Exine development in *Borago* (Boraginaceae). 2. Free microspore stages. *Taiwania* **44**: 212–229.

Sampathkumar A, Yan A, Krupinksi P, Meyerowitz EM. 2014. Physical forces regulate plant development and morphogenesis. *Current Biology* **24**: 475–483.

Scott RJ. 1994. Pollen exine – the sporopollenin enigma and the physics of pattern. In: Scott RJ, Stead MA, eds. *Society for Experimental Biology Seminar Series 55: Molecular and Cellular Aspects of Plant Reproduction.* Cambridge: Cambridge University Press, 49–81.

Sheldon JM, Dickinson HG. 1983. Determination of patterning in the pollen wall of *Lilium henryi*. *Journal of Cell Science* **63**: 191–208.

Shi J, Cui M, Yang L, Lim YJ, Zhang D. 2015. Genetic and biochemical mechanisms of pollen wall development. *Trends in Plant Science* **20**: 741–753.

Soltis DE, Soltis PS, Endress PK, Chase MW. 2005. *Phylogeny and evolution of angiosperms.* Sunderland, MA: Sinauer.

Taylor ML, Osborn JM. 2006. Pollen ontogeny in *Brasenia* (Cabombaceae, Nymphaeales). *American Journal of Botany* **93**: 344–356.

Taylor M, Cooper RL, Schneider EL, Osborn JM. 2015. Pollen structure and development in Nymphaeales: insights into character evolution in an ancient angiosperm lineage. *American Journal of Botany* **102**: 1–18.

Thompson DW. 1917. *On growth and form*. Cambridge: Cambridge University Press.

van Uffelen GA. 1991. The control of spore wall formation. In: Blackmore S, Barnes SH, eds. *Pollen and spores: patterns of diversification*. Oxford: Clarendon Press, 89–102.

Wang Y, Lin YC, So J, Du Y, Lo C. 2013. Conserved metabolic steps for sporopollenin precursor formation in tobacco and rice. *Physiologia Plantarum* **149**: 13–24.

Wang K, Guo Z-L, Zhou W-T, *et al.* 2018. The regulation of sporopollenin biosynthesis genes for rapid pollen wall formation. *Plant Physiology* **178**: 283–294.

Wehling K, Niester C, Boon JJ, Willemse MTM, Wiermann R. 1989. *p*-Coumaric acid – a monomer in the sporopollenin skeleton. *Planta* **179**: 376–380.

Wilmesmeier S, Wiermann R. 1997. Immunocytochemical localization of phenolic compounds in pollen walls using antibodies against *p*-coumaric acid coupled to bovine serum albumin. *Protoplasma* **197**: 148–159.

Wodehouse RP. 1935. *Pollen grains: their structure, identification and significance in science and medicine*. New York: McGraw-Hill.

Zhang ZB, Zhu J, Gao JF, *et al.* 2007. Transcription factor AtMYB103 is required for anther development by regulating tapetum development, callose dissolution and exine formation in *Arabidopsis*. *Plant Journal* **52**: 528–538.